

Sun-induced veiling glare in dusty camera optics

Carl Christian Liebe

Lawrence Scherr

Reg Willson

Jet Propulsion Laboratory
California Institute of Technology
4800 Oak Grove Drive
Pasadena, California 91109-8099

Abstract. The National Aeronautical and Space Administration (NASA) is planning to send two Mars Exploration Rovers (MER) to Mars in 2003. Onboard these rovers will be a number of scientific and engineering cameras. Mars is a dusty place, so dust will accumulate on the front surface of the camera optics. When the sun shines on the dusty front surface, light will be scattered to the detector. This increases glare and reduces contrast. The rover lenses must work, even when the sun shines on the front element. Therefore, the veiling glare has been evaluated by experiments. We discuss these experiments and the results.
© 2004 Society of Photo-Optical Instrumentation Engineers. [DOI: 10.1117/1.1635835]

Subject terms: Mars; Jet Propulsion Laboratory; Mars exploration rovers; camera; sun; veiling glare; dust; optics.

Paper 030186 received Apr. 21, 2003; revised manuscript received Sep. 5, 2003; accepted for publication Sep. 9, 2003.

1 Introduction

In early 2004, two highly capable Mars rovers will land on Mars. With far greater mobility than the 1997 Mars Pathfinder rover, these robotic explorers will be able to trek up to 100 m across the surface every Martian day. Each rover will carry a sophisticated set of instruments that will allow it to search for evidence of liquid water in the planet's past. The rovers will be identical to each other, but will land on different, equatorial regions of Mars.^{1,2}

The entry and landing is similar to the Pathfinder mission. First, the lander/rover separates from the cruise stage. Then, they will be captured by Mars using an aeroshell. A parachute will deploy in the atmosphere to slow the lander/rover. While the lander/rover is suspended in the parachute at an altitude of 1 to 2 km, a camera will image the Mars surface and determine the horizontal velocity. Rockets will then fire to slow the decent velocity and null the horizontal velocity. Airbags will inflate to cushion the landing, and the lander/rover will then be released from the parachute. On surface impact the airbags will bounce about a dozen times, and could roll as far as one kilometer. When they finally come to rest, the airbags will deflate and retract and the petals that surround the rovers will open, bringing the lander to an upright position and revealing the rover.¹

The landed portion of the mission is dramatically different from the Mars Pathfinder. Where Pathfinder had scientific instruments on both the lander and the small Sojourner rover, these larger rovers will carry all their instruments with them.

Each lander/rover will carry ten cameras. All cameras have identical detectors, electronics, interfaces, etc, but five different lens designs are employed. The imager is a 1024 × 2048-pixel frame transfer charge-coupled device (CCD) from Mitel (Wiltshire, UK).² The different cameras are as follows.

For Pancam, a stereo pair of 16-deg field-of-view panoramic cameras is mounted on top of the rover mast (Fig. 1). The stereo camera separation is 300 mm with 1-deg toe-in. The cameras each have a filter wheel with eight

positions. The rover mast gimbal mount can point the cameras in any orientation. The Pancams are used for scientific imaging and to image the sun for high-gain antenna pointing and north heading determination.³

For Navcam, a stereo pair of 45-deg field-of-view navigation cameras is also mounted on the top of the rover mast. The camera separation is 200 mm, and they are pointed similar to the Pancams. The Navcams provide long-range viewing of the terrain around the rover for use by ground operators in planning rover traverses. These cameras may also be used by on-board navigation algorithms to assist in autonomous navigation, or for general monochromatic imaging. They also support the science operations of near-field target selection and viewing some of the workspace of the rover's instrument arm.

A microscopic imager camera is mounted on the end of a moveable arm. This camera is used to acquire closeup images of geological features. By moving the camera, pairs of images may be combined into stereo images. The microscopic imager includes a dust cover that will reduce the amount of dust that accumulates on the optics. Also, the

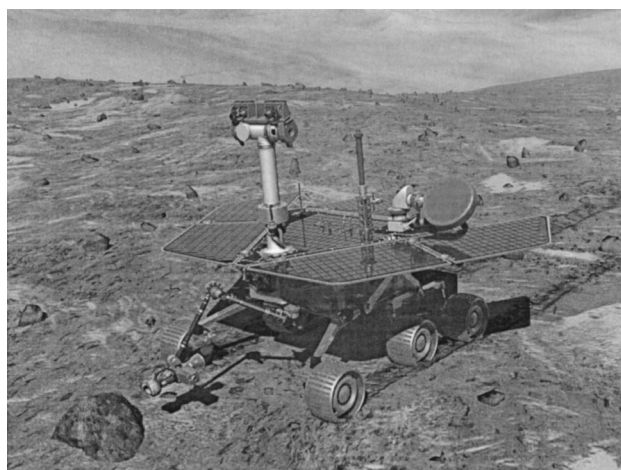


Fig. 1 An artist's image of the MER rover on the Mars surface.

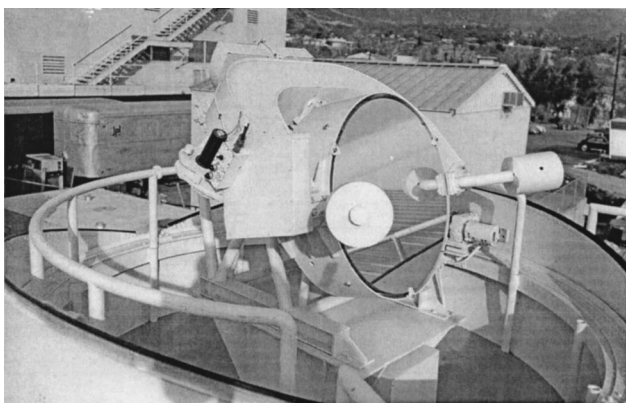


Fig. 2 The heliostat at JPL.

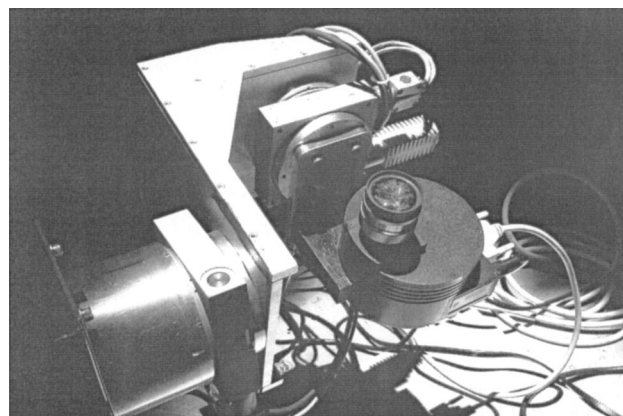


Fig. 4 Sun-illuminated lens mounted in goniometer.

microscopic imager front lens is almost always shaded from the sun by the rocks or the rover. Glints off the dust cover might be a problem if the cover reflects sun back to the lens. However, moving the arm can mitigate this.

A set of stereo hazard avoidance cameras, Hazcams, is mounted near the wheels on front and back of the rover. The separation between the cameras is 100 mm and the field of view is 124 deg. The Hazcams provide imaging, primarily of the near field around the rover (<5 m), both in front of and behind the rover. These cameras will aid in determining a safe egress direction for the rover. They provide the data for on-board hazard detection using stereo imaging to build range maps. Finally, they support science operations for selecting near-field target and instrument deployment mechanism operations.

The descent camera is mounted on the lander looking down. It is a modified Navcam that is used to measure the horizontal velocity of the lander during the final phase of the decent. Correlating features on the surface in consecutive images determine the horizontal velocity. Thrusters reduce the horizontal velocity for safe airbag landing.

Mars has fine $\sim 1\text{-}\mu\text{m}$ dust suspended in the atmosphere. Dust settles out of the atmosphere at a rate that depends on the geographical position and time of the year.⁴ Estimates of the settling rate predict that obscuration of a horizontal surface (like a solar panel) are 0.3% per Martian day.⁵ Martian dust will accumulate more slowly on protected vertical surfaces like rover camera lenses.

Pancams and Navcams, when imaging, present a vertical surface to dust settling from the Martian atmosphere. At



Fig. 3 The lens used for testing in this work.

least once a day they will be turned toward zenith to find the sun for recalibrating navigation. They can be pointed down when not in use to limit dust accumulation. They will need to image with sunlight shining on their front lens.

Hazcams may be exposed to dust from the wheels, saltation, or rock abrasion. They are almost always shaded from the sun because they are under the solar panels, shown in Fig. 1.

The microimager camera may be exposed to dust from rock abrasion. It will almost never be imaging with sunlight shining on the front lens.

2 Experimental Equipment

The heliostat facility at the Jet Propulsion Laboratory (JPL) was used to provide a controlled sun bundle for the veiling glare measurements. The facility contains a heliostat, which is simply a “sun tracker.” The heliostat consists of a large mirror sitting on a two-axis gimbal inside a dome attached to the facility. The sun is tracked by this gimbal system and the sunbeam is directed toward a fixed mirror located on the ceiling of the facility. This makes a 3-foot-diam sunbeam pointing straight down inside the laboratory for about 4 to 6 h around noon time (depending on the season). A picture of the heliostat is shown in Fig. 2. A camera for glare testing was placed in the heliostat sunbeam.

An off-the-shelf video C-mount lens was selected as a stand-in for Mars exploration rover (MER) lenses, because the MER lenses were not available for contamination and stray-light testing. The lens barrel is marked “Videostigmat, F/1.0, 1.5 inch, Carl Meyer.” The lens diameter is 48 mm and the focal length is 38.1 mm. The iris was stopped down slower than F/11, $\sim 2\text{-mm}$ aperture diameter. The rim of the lens barrel is only 3 mm out from the front lens element. An image of the dust-contaminated lens is shown in Fig. 3.

The camera CCD is a Kodak KAF-401E. It is fitted in a commercial SBIG 7I CCD camera.⁶ Camera images are stored on a computer.

The lens and camera system was mounted in a computer-controlled goniometer so CCD images could be recorded as a function of sun illumination angle. The heliostat directed sunlight down onto the goniometer. Goniometer angles were defined so the sun was illuminating the lens along the optical axis for a 0-deg goniometer angle.

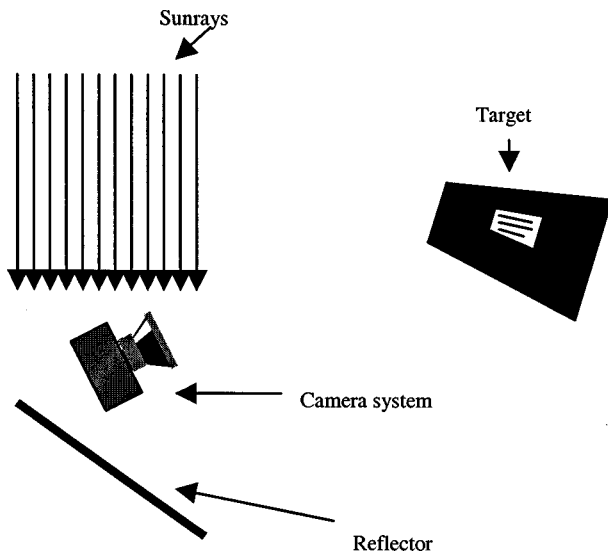


Fig. 5 Sketch of the setup.

The goniometer and lens are shown in Fig. 4. The shadow below the lens shows the angle of incidence (AOI) is about 30 deg in this picture.

3 Experimental Determination of Contrast in Dust-Contaminated Lenses

Observing a sun-illuminated scene, with and without sun-induced veiling glare, can help us interpret the veiling glare compared to the expected signal. Therefore, images of a sun-illuminated sheet of paper with alternating white and black bars were acquired as a model scene. The camera was sun illuminated at a 60-deg AOI. A shiny sheet metal panel was used as a mirror to reflect the sunbeam to illuminate the paper at near normal incidence. This setup is sketched in Fig. 5. Images were collected with either a bare dusty lens illuminated by sunlight, or a completely shaded dusty lens (Figs. 6 and 7). The sun-illuminated page saturated the

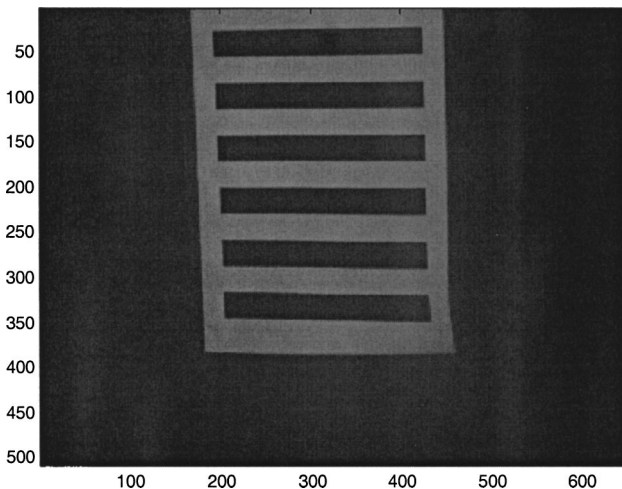


Fig. 6 Image of the bar target. The sun does not hit the dust-contaminated lens front surface. The dust contamination level is 46% transmission relative to no contamination.

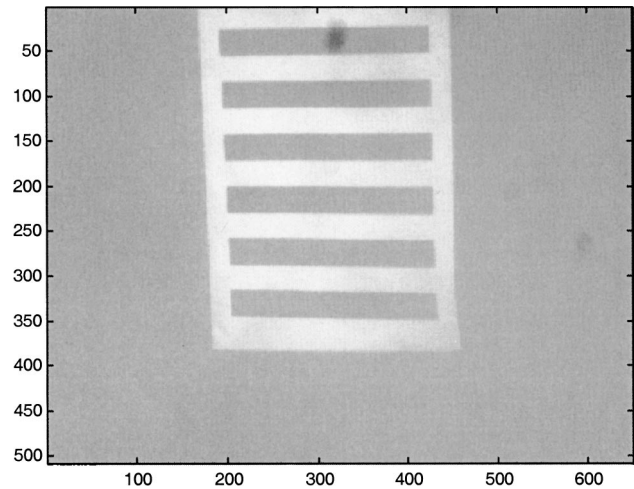


Fig. 7 Image of the bar target. Sun illuminates the dust-contaminated lens front surface. The dust contamination level is 46% transmission relative to no contamination.

CCD, so a 50% attenuating neutral density filter (ND 0.3) filter was placed in front of the lens for these measurements.

Images were recorded with five different levels of dust contamination. For the different levels of dust contamination, a pixel count of the white areas of the image was measured. The ratio of contaminated to clean pixel count is a measure of transmission through the dust. The five different levels of dust contamination gave 100, 83, 77, 65, and 46% transmission.

The front element of the lens was either illuminated by sunlight with 60-deg AOI, or completely shaded from the sun. A bar target image for the dusty shaded lens is shown in Fig. 6. Pixel count profiles through the white and black bars of the images were calculated and are shown in Fig. 8 for the shaded lens.

A bar target image for the dusty unshaded lens is shown in Fig. 7. Dust contamination corresponds to 46% transmission. A pixel count profile of the image (through the bar target) is shown in Fig. 9. Figures 8 and 9 also show the profile curves for other levels of dust contamination. Veiling glare introduces a significant background glow for the sun-illuminated lens. The minimum pixel count background increases dramatically with contamination. When the dust contamination level reduces transmission to 46%, the veiling glare is several times stronger than the signal itself. This will make imaging and detection of weak signals difficult. Also, a significant part of the CCD potential well will be filled with veiling glare. This reduces the dynamic range of the pixel.

Bar target modulation is defined as $(\max - \min) / (\max + \min)$. For the shaded lens, the maximum pixel count decreases while the minimum stays about the same as contamination increases (transmission goes down) ($\max - \min$) decreases because transmission decreases through the dusty lens. Modulation decreases slowly as contamination increases for the shaded lens (Table 1).

For the sun illuminated lens, $(\max - \min)$ is about the same as for the shaded lens, for each contamination level. $(\max - \min)$ is a measure of reflectance ratio between black

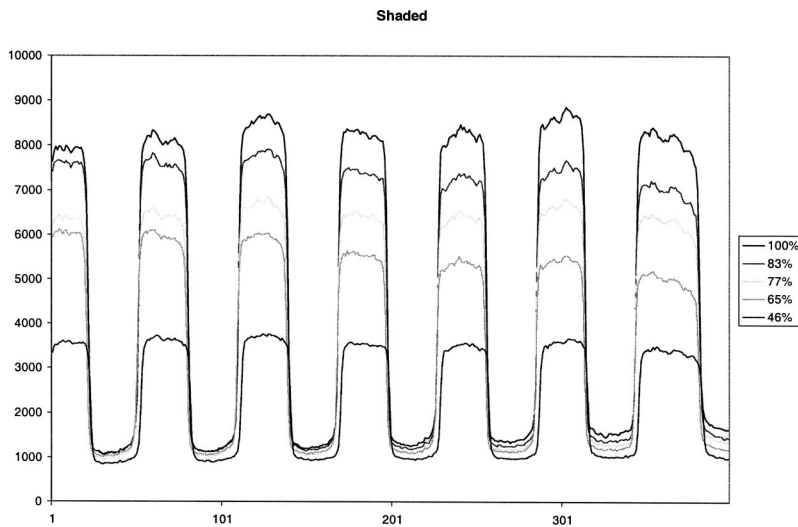


Fig. 8 The contrast in the image, when the lens was shaded.

and white bars. The pixel counts for both white and black bars increase, because contamination increases the amount of sunlight scattered from the lens. Modulation for the sun-illuminated lens decreases more dramatically as contamination increases (Table 1).

Stray light from scatter off the sun-illuminated front lens is only troublesome if it is comparable to CCD counts from the sun-illuminated Mars scene. The sun illuminated printed paper page is a model for the sun-illuminated Mars scene. Stray light from the sun-illuminated lens reduces scene contrast (Fig. 7), compared to the contrast when the lens is shaded (Fig. 6).

4 Experimental Evaluation of Veiling Glare Mitigation Utilizing a Sunshade

One technique to avoid veiling glare is to shield the lens front surface from sunlight using a sunshade. Therefore, an experimental characterization of the veiling glare was done as a function of AOI for different lengths of sunshade.

In the experiment, images versus sun AOI were recorded for the bare lens and with a short and long sunshade. The sunshade was black paper wrapped around the lens barrel. The short sunshade was 14.3 mm out from the front lens surface. The long shade was 27 mm deep. Shade diameter was 48 mm. The shades are shown with a dusty lens in Fig. 10.

Very fine rock dust powder, prepared by JPL to model the dust from the Rock Abrasion Tool (RAT droppings, Palisades Basalt), was dusted uniformly over the lens to simulate Mars dust on a rover lens. The dust was like fine flour. Particle size distribution is unknown.

Veiling glare was measured as a function of sun angle, with and without a sunshade and with and without dust on the lens. Image contrast was measured as a function of different levels of dust on the lens.

Average and maximum pixel counts are plotted as a function of AOI for a clean bare lens (Fig. 11). The curves show a saturated flat-top plateau for 0- to 25-deg AOI.

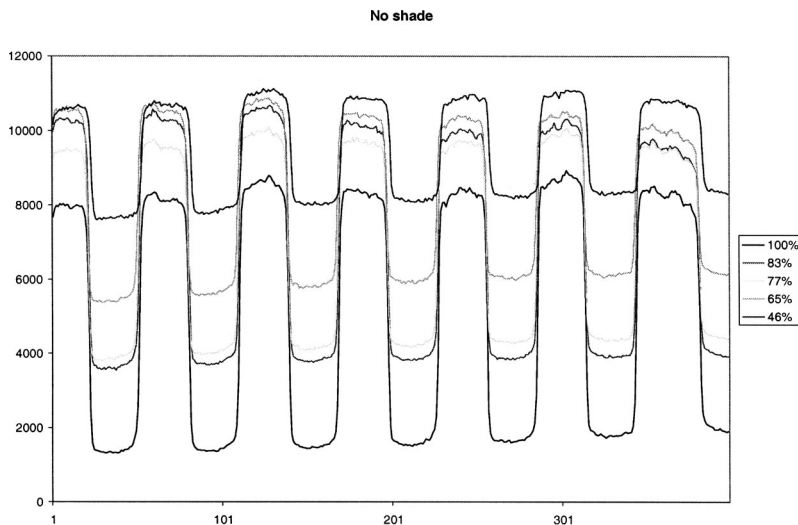


Fig. 9 The contrast in the image acquired with a sun-illuminated lens.

Table 1 Contrast decreases more rapidly with contamination for the sun-illuminated lens.

Transmission of contaminated lens	Shaded lens modulation	Sun illuminated lens modulation
100%	74%	69%
83%	72%	44%
77%	71%	40%
65%	65%	27%
46%	59%	15%

Counts drop below saturation at 25-deg AOI. Average counts form a shoulder at 25- to 40-deg AOI, then fall to near background level for 45- to 85-deg AOI. Maximum pixel counts are just slightly higher than average counts, except they are considerably higher over the 25- to 45-deg shoulder. Curves for the clean lens with short (14.3 mm) sunshade (Fig. 12) are almost the same as for no shade. Finally, curves for the clean lens with long (27 mm) shade

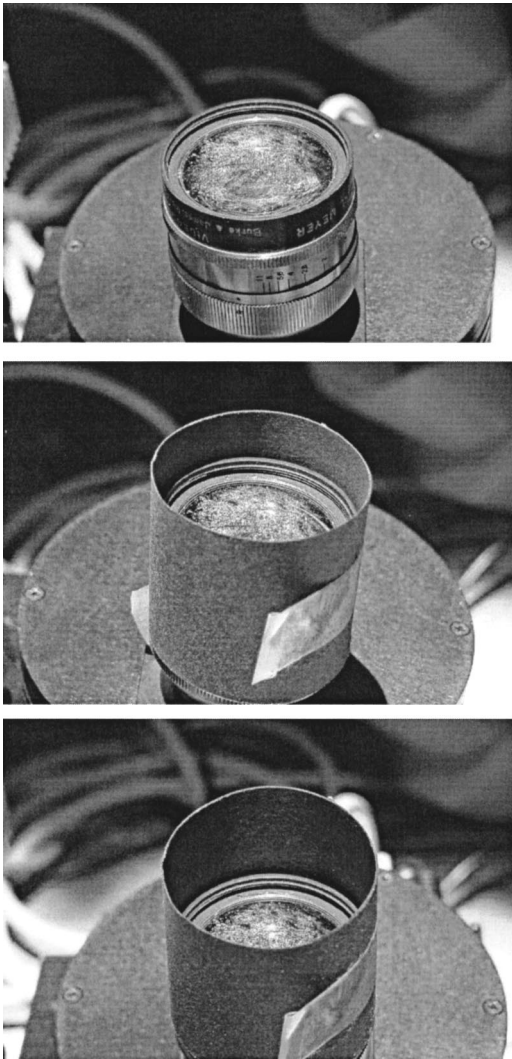


Fig. 10 Dusty lens with different length sunshade.

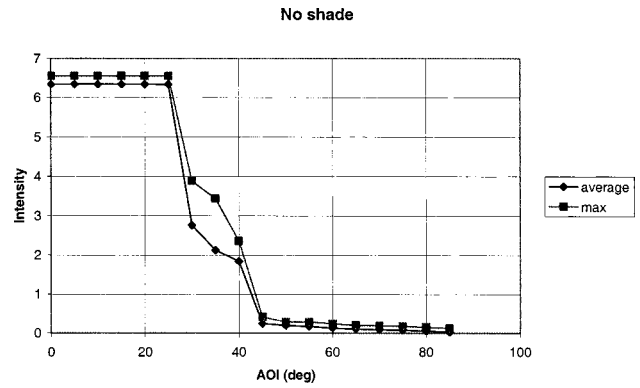


Fig. 11 Clean lens with no sunshade.

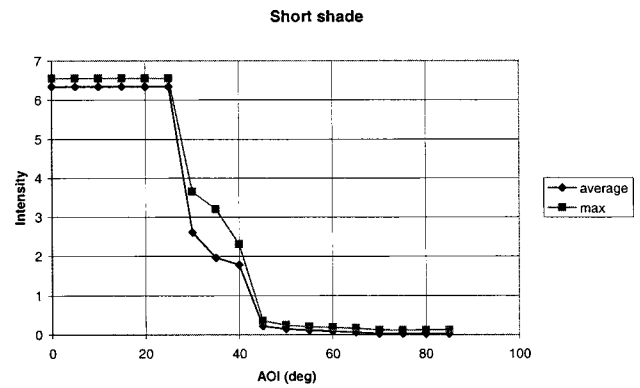


Fig. 12 Clean lens with short sunshade.

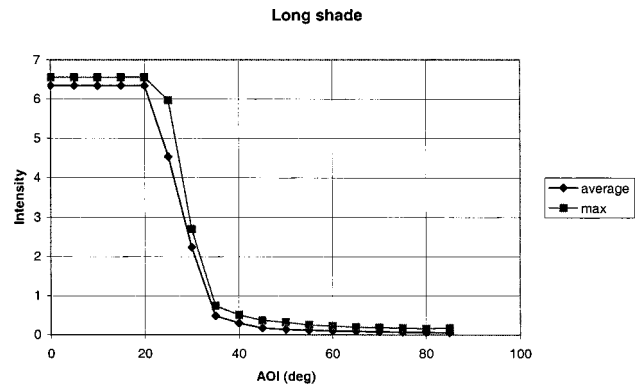


Fig. 13 Clean lens with long sunshade.

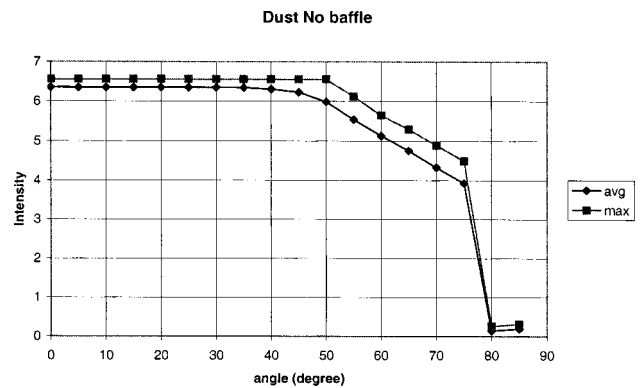


Fig. 14 Dusty lens with no sunshade.

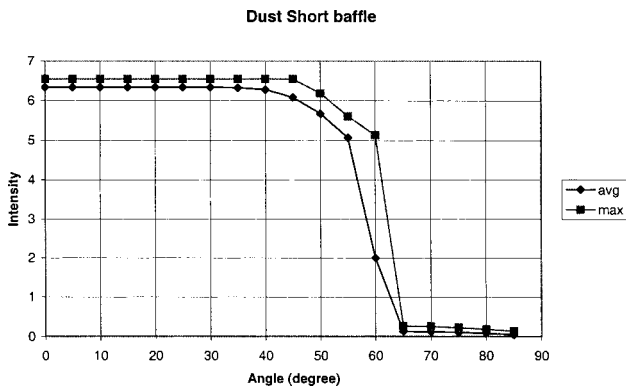


Fig. 15 Dusty lens with short sunshade.

(Fig. 13) show a saturated flat top plateau for 0 to only 20-deg AOI. Counts drop from 25 to 40 deg and are near background from 45- to 85-deg AOI.

Curves for the dusty lens with no sunshade (Fig. 14) show a saturated flat-top plateau for 0- to 40-deg AOI. Counts drop gradually over 45 to 75 deg, and then drop to near background level at 80- to 85-deg AOI. Curves for the dusty lens with short sunshade (Fig. 15) show a flat-top plateau for 0- to 40-deg AOI. Counts drop gradually over 45 to 55 deg, and then drop to near background level at 65- to 85-deg AOI. Curves for the dusty lens with long sunshade (Fig. 16) show a flat-top plateau for 0- to 35-deg AOI. Counts drop rapidly over 40 to 45 deg. Counts are near background level at 45- to 85-deg AOI.

The pixel counts versus AOI curves (Figs. 11–16) were recorded in the JPL celestial simulator facility, which has black, featureless, low-reflectance walls. At goniometer angles above 20-deg AOI, the camera was looking at the black walls. At these goniometer angles, the pixel counts above background are a measure of veiling glare.^{7,8}

The curves show a flat-top plateau, because intensity is near saturated for 0- to 25-deg AOI. Maximum pixel counts are just slightly higher than average counts, because the glare is rather uniform for 45- to 85-deg. AOI. The glare has ghost reflection structure and bright spots for 0- to 40-deg AOI. Saturation keeps maximum counts just slightly above average for 0-to 20-deg AOI. Falling out of saturation allows the bright spot maximum to be considerably higher than average counts over the 25-to 40-deg plateau.

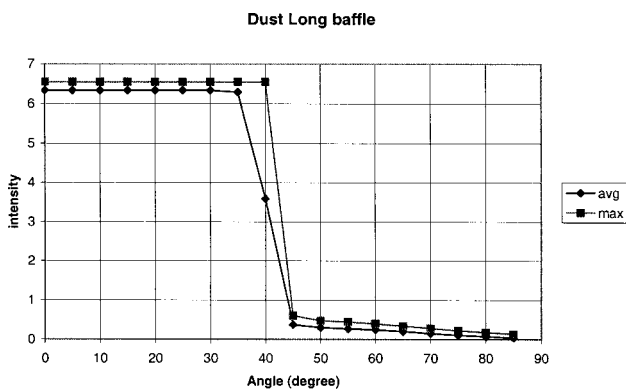


Fig. 16 Dusty lens with long sunshade.

The short (14.3 mm) sunshade blocks sunlight from the lens center at angles above ~59-deg AOI. This is calculated from sunshade length and semidiameter [$\text{inverse tan } 14.3/(48/2) = 31 \text{ deg}$, $\text{AOI} = 90 \text{ to } 31 \text{ deg} = 59 \text{ deg}$]. Ghosts are already gone at this angle. Even a lens with no shade has reached background at angles above 45-deg AOI. This may explain why the short shade and no shade curve look the same.

The long (27 mm) sunshade blocks sunlight from the lens center at angles above ~42-deg AOI [$\text{inverse tan } 27/(48/2) = 48 \text{ deg}$, $\text{AOI} = 90 \text{ to } 48 \text{ deg} = 42 \text{ deg}$]. The upper portion of the lens is shaded at a smaller AOI. This may reduce ghosts and explain the drop from 25 to 40 deg with no plateau (Fig. 12).

The dusty lens front surface scatters much more sunlight back through the lens to the CCD, compared to the clean lens. The flat-top plateau persists out to 40-deg AOI (Fig. 14), compared to 25 deg for the clean lens. The gentle slope from 50 to 75 deg may be related to the bidirectional reflectance distribution function (BRDF) curve for the dusty front lens. The sharp drop from 75 to 80 deg is because the goniometer structure and rim of the lens barrel are shading the lens center. The short sunshade blocks sunlight from the lens center at angles above ~59-deg AOI, with the upper portion of the lens shaded at even smaller AOI. This explains the sharp drop from 55 to 65 deg (Fig. 15). The long sunshade blocks sunlight from the lens center at angles above ~42-deg AOI, with the upper portion of the lens shaded at even smaller AOI. This explains the sharp drop from 35 to 45 deg (Fig. 16).

5 Summary

We describe the upcoming NASA Mars exploration rover mission. Since Mars is a dusty place, there has been concern on how the cameras would perform with Mars dust on the front surfaces.

Two experiments are done. In the first experiment, a bar target is imaged with various degrees of dust contamination on the lens. The images are acquired with and without sun illumination on the front surface of the lens. The experiment shows that the sun introduces a significant background glow in the image, if the lens is contaminated.

One way to mitigate the sun-induced veiling glare is to use a sunshade on the lens. The second experiment therefore characterizes the veiling glare as a function of the sun angle for different designs of sunshades. The experiments show that veiling glare is significantly reduced if the sun is not illuminating the front surface of the lens directly.

Questions about how sun illuminations would affect the camera performance on the MER rovers motivated this study. The preliminary results of this study resulted in all camera positions and orientations being assessed relative to the sun. As a result, a sunshade was added to the Navcam cameras to avoid the sun would be shining on the optics for a majority of the time.

Acknowledgments

The research described here was carried out at the Jet Propulsion Laboratory, California Institute of Technology, under a contract with the National Aeronautics and Space Administration. References herein to any specific commercial

product, process, or service by trademark, manufacturer, or otherwise, do not constitute or imply its endorsement by the United States Government or the Jet Propulsion Laboratory, California Institute of Technology.

References

1. Jet Propulsion Laboratory, California Institute of Technology, see <http://www.jpl.nasa.gov/missions/future/marsexplorationrovers.html> (2001).
2. A. R. Eisenman, C. C. Liebe, M. Maimone, M. A. Schwochert, and R. G. Willson, "Mars exploration rover engineering cameras," *Proc. SPIE* **4540**, 288–297 (2001).
3. G. H. Smith, E. C. Hagerott, L. M. Scherr, K. E. Herkenhoff, and J. F. Bell III, "Optical designs for the Mars '03 rover cameras, current developments in lens design and optical engineering," *Proc. SPIE* **4441**, 118–131 (2001).
4. H. A. Perko, J. D. Nelson, and J. R. Green, "Review of martian dust composition, transport, deposition, adhesion, and removal," *Proc. Space 2002, The Eight International Conference on Engineering, Construction, Operations and Business* **176**(14) (2002).
5. G. A. Landis, "Materials adherence experiment results from Mars Pathfinder," *Proc. 26th IEEE Photovoltaic Specialists Conf.*, pp. 865–869 (1997).
6. Santa Barbara Instrument Group, Santa Barbara, USA, see <http://www.sbig.com/sbwhtmls/online.htm> (2002).
7. ANSI PH3.615, Lens and lens systems method for testing veiling glare.
8. ISO 9358, "Optics and optical instruments, Veiling glare of image forming systems, Definitions and methods for measurement," publication date 07/14/1994, ISO/TC 172/SC1

Carl Christian Liebe received his MSEE degree in 1991 and the PhD degree in 1994 from the Department of Electrophysics, Technical University of Denmark. Since 1997, he has been with the Jet

Propulsion Laboratory, California Institute of Technology. Currently, he is a senior member of the technical staff in the Precision Motion Control Systems and Celestial Sensors Group. He has more than 10 years of experience in star trackers, sun sensors, target tracking, and image processing. His current research interests include miniaturization of attitude determination sensors. He has authored and coauthored more than 40 papers.

Lawrence Scherr is an optical engineer and lens designer. He received his MS in physics from University of Illinois, Urbana, in 1972. He received his PhD in biophysics from University of California, Berkeley, in 1980. He has designed, built, tested, or analyzed stray light on an enjoyable variety of optics. These include prototype medical instruments, intraocular lenses, scatterometers, large surveillance telescopes, automated optical test systems, and Mars camera lenses.

Reg Willson is a Senior Member of Technical Staff in JPL's Machine Vision Group. In addition to working on the 2003 Mars exploration rover cameras, he is involved with developing slope navigation technologies for future rover missions. His research interests include camera modeling and calibration, computer vision, electronic imaging, and real-time systems. He received his MS (1988) and PhD (1994) in electrical engineering from Carnegie Mellon University. His thesis research concentrated on modeling and calibration of automated zoom lenses for machine vision and robotics. In March 1994, he joined 3M's Engineering Systems Technology Center in Saint Paul, Minnesota, where he developed optical inspection systems and technology for 3M manufacturing. In April 2001, he moved to California to join the NASA Jet Propulsion Laboratory, California Institute of Technology.